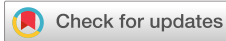


RESEARCH ARTICLE | OCTOBER 25 2023

Effects of rotational excitation on decay rates of long-lived Rydberg states in NO

M. H. Rayment ; S. D. Hogan  



J. Chem. Phys. 159, 164309 (2023)

<https://doi.org/10.1063/5.0171329>



View
Online



Export
Citation

CrossMark

Effects of rotational excitation on decay rates of long-lived Rydberg states in NO

Cite as: J. Chem. Phys. 159, 164309 (2023); doi: 10.1063/5.0171329

Submitted: 8 August 2023 • Accepted: 6 October 2023 •

Published Online: 25 October 2023



View Online



Export Citation



CrossMark

M. H. Rayment  and S. D. Hogan ^{a)} 

AFFILIATIONS

Department of Physics and Astronomy, University College London, Gower Street, London WC1E 6BT, United Kingdom

^{a)} Author to whom correspondence should be addressed: s.hogan@ucl.ac.uk

ABSTRACT

Nitric oxide (NO) molecules in pulsed supersonic beams have been excited to long-lived Rydberg-Stark states in series converging to the lowest vibrational level in the ground electronic state of NO⁺ with rotational quantum numbers $N^+ = 2, 4,$ and 6 . The molecules in these excited states were then guided, or decelerated and trapped in a chip-based Rydberg-Stark decelerator, and detected *in situ* by pulsed electric field ionization. Time constants, reflecting the decay of molecules in $N^+ = 2$ Rydberg-Stark states, with principal quantum numbers n between 38 and 44, from the electrostatic traps were measured to be $\sim 300 \mu\text{s}$. Molecules in Rydberg-Stark states with $N^+ = 4$ and 6 , and the same range of values of n were too short-lived to be trapped, but their decay time constants could be determined from complementary sets of delayed pulsed electric field ionization measurements to be ~ 100 and $\sim 25 \mu\text{s}$, respectively.

© 2023 Author(s). All article content, except where otherwise noted, is licensed under a Creative Commons Attribution (CC BY) license (<http://creativecommons.org/licenses/by/4.0/>). <https://doi.org/10.1063/5.0171329>

I. INTRODUCTION

High Rydberg states of small molecules are of interest in precision tests of molecular quantum mechanics,^{1–5} studies of photoionisation dynamics and plasma recombination,^{6–11} investigations of long-range interactions with other atoms and molecules and the formation of exotic bound states,^{12–14} and studies of ion-molecule reactions at low temperatures.^{15–18} The preparation of cold electrostatically trapped gases of such molecules offers opportunities to study slow excited-state decay processes, including effects of weak intramolecular interactions, with unprecedented precision on the order of 1 kHz.^{19–21} Investigations of effects of rotational and vibrational excitation on these Rydberg state decay rates provide valuable input into the development of new approaches to trace gas detection.^{22,23}

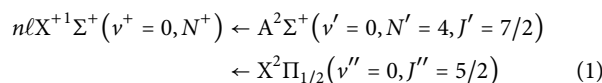
Here we demonstrate the use of a combination of the methods of Rydberg-Stark deceleration and electrostatic trapping, and delayed pulsed electric field ionization (PFI) to study effects of rotational excitation of the NO⁺ ion core on the decay of long-lived Rydberg states in Nitric oxide (NO). The states studied had rotational quantum numbers of the ion core of $N^+ = 2, 4,$ and 6 . The measurements reported extend beyond previous work in which effects of vibrational excitation on slow decay processes of long-lived Rydberg states in NO in series with $N^+ = 0, 1,$ and 2 were

studied.^{19–21} That earlier work allowed bounds to be placed on effects of vibrational autoionization on the decay of such states.

In the following, the experimental apparatus and techniques are described in Sec. II. The results of the experiments are then presented and discussed in Sec. III. In Sec. IV conclusions are drawn.

II. EXPERIMENT

The experiments described here were carried out in a cryogenically cooled chip-based Rydberg-Stark deceleration apparatus.^{19,20} In this setup, pure pulsed supersonic beams of NO were generated with a mean longitudinal speed of 800 ms^{-1} . The molecules in these beams were photoexcited from the negative-parity lambda-doublet component of the X²Π_{1/2} ground electronic state with $J'' = 5/2$, to high Rydberg states using the resonance-enhanced



two-color two-photon excitation scheme,^{24–26} as depicted in Fig. 1. This was driven using the frequency tripled and frequency doubled outputs of two counter-propagating Nd:YAG-pumped pulsed dye lasers at wavenumbers ν_1 and ν_2 , respectively. For the measurements

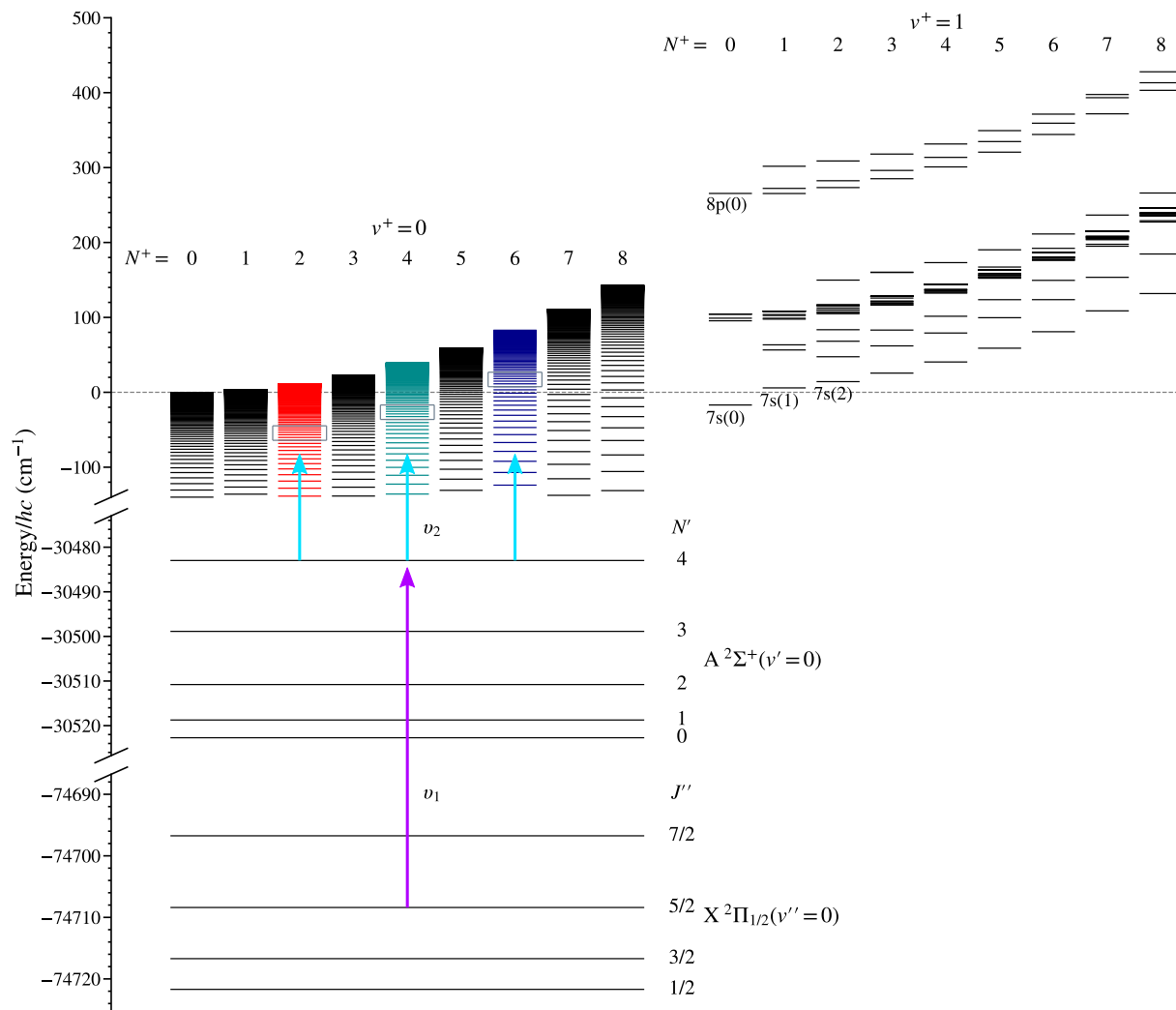


FIG. 1. Resonance-enhanced two-color two-photon laser excitation scheme used to prepare high- n Rydberg states in NO, in series converging to the $v^+ = 0$ vibrational level in the ground electronic state of NO⁺ with rotational quantum numbers $N^+ = 2, 4,$ and 6 . The grey rectangles overlaid on the Rydberg series on the left side of the figure encompass the energetic regions containing the Rydberg states with values of n between 38 and 44 studied here. Short lived $n = 7$ states in Rydberg series with $v^+ = 1$ that are located close to the $v^+ = 0, N^+ = 0$ ionization limit are indicated on the right side of the figure. In the wavenumber range encompassed in this part of the figure, the states with all possible values of ℓ and N are included but not explicitly labelled.

reported here $\nu_1 = 44\,225.35\text{ cm}^{-1}$ ($\equiv 226.115\text{ nm}$) [$\sim 90\ \mu\text{J/pulse}$], and ν_2 was tuned in the range from $30\,384$ to $30\,511\text{ cm}^{-1}$ ($\equiv 329.12\text{--}327.75\text{ nm}$) [$\sim 0.7\text{ mJ/pulse}$]. The radiation at wavenumber ν_1 (ν_2) was linearly polarized parallel (perpendicular) to the axis of propagation of the molecular beam. For each laser system the vacuum wavelength of the fundamental output was monitored and calibrated using a fibre-coupled wavelength meter. The intensity of the tunable radiation at wavenumber ν_2 was monitored on a photodiode.

After photoexcitation, three types of measurements were performed. Either the Rydberg molecules: (i) travelled for a short distance beyond the excitation position for a time $t = 1\ \mu\text{s}$ before

detection by pulsed electric field ionization (PFI); (ii) were loaded into a single traveling electric trap of the Rydberg-Stark decelerator²⁷ and guided at a constant speed of 795 ms^{-1} to a detection position $\sim 10\text{ cm}$ downstream in the apparatus, with delayed PFI then performed at a time $t = 132\ \mu\text{s}$ after photoexcitation; or (iii) were decelerated in a traveling trap in the decelerator from 795 ms^{-1} to rest in the laboratory-fixed frame of reference. In this last case detection of the trapped molecules was carried out *in situ* at the position of the trap by PFI at times $t \geq 250\ \mu\text{s}$ after photoexcitation.²⁸ The PFI process was implemented with a rapidly-rising pulsed potential applied to one of the electrodes in the excitation region (measurement type i), or the side electrodes in the decelerator (measurement

types ii and iii), or in a state-selective way (SFI) using a slowly rising potential. The SFI potential had a rise time of $\sim 4.4 \mu\text{s}$ corresponding to a switching rate of $\sim 70 \text{ V}/\mu\text{s}$, and allowed electrons produced by direct photoionization to be distinguished from those generated by electric field ionization of bound Rydberg states. The ions or electrons generated by PFI or SFI were accelerated out of the decelerator structure and cryogenic region of the apparatus and collected at either one of two microchannel plate (MCP) detectors operated at room temperature. The operating potentials of the MCPs were adjusted to allow NO^+ ion detection by PFI, or electron detection by SFI.

III. RESULTS AND DISCUSSION

The photoexcitation scheme in Eq. (1) goes through the intermediate A state with total angular momentum quantum number excluding spin $N' = 4$. This state is a low-lying Rydberg state with 94% s character and 5% d character.^{29,30} Single photon electric dipole transitions from this state to high- n Rydberg states may be considered, within the ion-core rotation spectator model, to transfer all photon angular momentum to the excited electron. This allows optical access to Rydberg states with np or nf character. The np Rydberg states in NO decay rapidly by predissociation. Therefore, the longer-lived states of interest in the experiments reported here were those with nf character. In the high- n Rydberg states, the rotational angular momentum vector of the ion core excluding spin is $\vec{N}^+ = \vec{N} - \vec{\ell}$. As the rotational angular momentum of the ion core remains unchanged in the transition $\vec{N}^+ = \vec{N}' - \vec{\ell}'$, where $\vec{\ell}'$ is the electron orbital angular momentum vector in the A state, and therefore $N^+ = |N' - \ell'| \dots |N' + \ell'|$.³¹ However, since these Rydberg states must be of opposite parity to the intermediate A state, when excited in a single-photon electric dipole transition, and the $A^2\Sigma^+(v' = 0, N' = 4, J' = 7/2)$ state has positive parity, only Rydberg states for which $(-1)^{N^+ + \ell} = -1$ are optically accessible. These are therefore the nf Rydberg states for which $N^+ = 2, 4,$ and 6 .

In the experimental apparatus, weak time-varying electric fields associated with laboratory noise, and collisions with ions and electrons present close to the time of laser photoexcitation, gave rise to population transfer from the field-free nf Rydberg states into longer-lived ℓ -mixed Rydberg-Stark states.^{32,33} This process occurred most effectively for states with nf character because of their comparatively small quantum defects of $\delta_r \approx 0.02$,^{34,35} and hence their energetic proximity to the higher- ℓ states with the same value of n . This ℓ -mixing happened less readily for the shorter-lived np states, particularly at lower values of n , because of their larger quantum defects of $\delta_p \sim 0.7$.^{26,36} The Rydberg-Stark states populated by this mechanism in the experiments may be considered hydrogenic states. Their electronic wavefunctions have approximately equal amplitude contributions from orbitals with all values of $\ell \geq 3$, and they exhibit linear Stark energy shifts in weak electric fields. The particular subset of these levels with positive Stark shifts, i.e., the low-field-seeking states, are well suited to deceleration and electrostatic trapping using inhomogeneous electric fields.³⁷ Because the quantum defects of the nf states are not strongly dependent on the rotational quantum number, N^+ , of the NO^+ ion core, the mechanisms by which the long-lived Stark states are populated are similar for Rydberg series

with different values of N^+ . By exciting the molecules through the level in the intermediate A-state with a rotational quantum number $N' = 4$, it was therefore possible to prepare molecules in similar distributions of ℓ -mixed Rydberg-Stark states in series with $N^+ = 2, 4,$ and 6 .

The spectrum of Rydberg states prepared in the experiments, with lifetimes sufficient for detection $1 \mu\text{s}$ after excitation, can be seen in Fig. 2(c). This was recorded by SFI, to allow the signal from the bound Rydberg states presented, to be separated from that of free electrons generated by direct photoionisation close to, or above the series limits for the lower values of N^+ . This, and the other spectra in Fig. 2, represent the mean of between 7 and 16 individual spectra. When recording these spectra, the intensity and wavenumber of ν_2 was monitored for each data point. The NO^+ ion, or the electron signal on the MCP was then normalized to account for effects of shot-to-shot intensity fluctuations by dividing by the laser intensity. Since the sets of values of ν_2 sampled in each individual spectrum were not exactly the same from one measurement to the next, because of the way in which the tunable dye laser was scanned, to average the spectra, an equally spaced set of wave numbers covering the entire measurement range was generated. At each wavenumber in this set, the average spectral intensity was then determined from the weighted mean of the individual spectra using a Gaussian weighting function with a standard deviation $\sigma = 0.075 \text{ cm}^{-1}$ corresponding to that of the laser spectral profile.

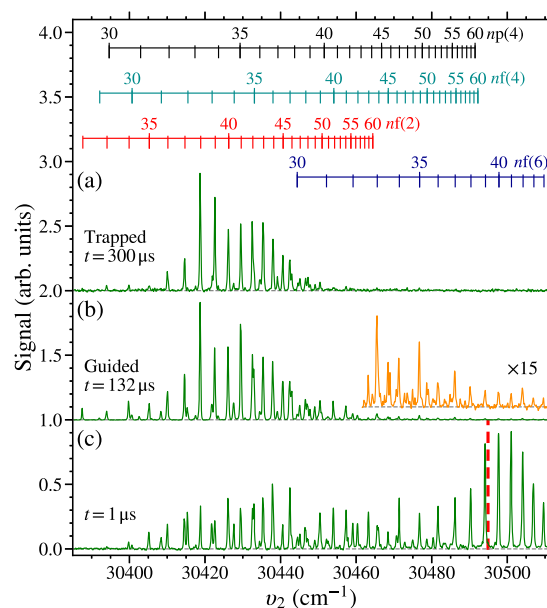


FIG. 2. Laser photoexcitation spectra of Rydberg states in NO recorded after (a) deceleration and trapping at $t = 300 \mu\text{s}$, (b) transport at constant speed in a traveling electric trap in the decelerator with detection at $t = 132 \mu\text{s}$, and (c) detection at $t = 1 \mu\text{s}$ after photoexcitation. For all measurements, $\nu_1 = 44\,225.35 \text{ cm}^{-1}$. The vertical red dashed line at $30\,494.90 \text{ cm}^{-1}$ in (c) indicates the $N^+ = 2$ series limit. The spectra in (a) and (b) were recorded by monitoring the NO^+ ion signal following delayed PFI. The spectrum in panel (c) was recorded by electron detection following SFI.

The spectrum in Fig. 2(c) contains transitions to states with values of n between 33 and ~ 55 in the $N^+ = 2$ (lowest wavenumber resonances), $N^+ = 4$ (middle section of the spectrum between $\sim 30\,430$ and $30\,480\text{ cm}^{-1}$), and $N^+ = 6$ (high wavenumber resonances) series. Each of the features observed can be associated with transitions to the individual Rydberg states in these series as indicated by the vertical bars at the top of the figure. The series observed are those expected from the propensities for transitions from the intermediate A state.^{31,38} The spectra are dominated by transitions to $n\ell(N^+) = nf(N^+)$ Rydberg states. However, there are several features corresponding to excitation on $np(4)$ resonances. These typically arise as a result of intramolecular charge-multipole interactions between near degenerate states.^{26,35,39} Interactions of this kind mix optically accessible $np(4)$ character into $n'\ell'(N^+')$ states which further evolve in the time-varying electric fields close to the time of excitation into long-lived $n'(N^+')$ ℓ -mixed Rydberg-Stark states. The intensities of the resonances observed depend on the efficiency with which the Rydberg-Stark states are populated in each case. The increase in the intensity of the signal associated with the excitation of $N^+ = 6$ states with values of $n > 38$ and $\nu_2 > 30\,490\text{ cm}^{-1}$ is attributed to an increase in the number of ions and electrons, and enhanced electric-field-induced ℓ - and M_N -mixing close to the time of photoexcitation, in this spectral region which is close to or above the $N^+ = 2$ series limit (dashed red vertical line).

The spectrum in Fig. 2(b) was recorded by detection of molecules that were loaded into a single traveling electric trap in the Rydberg-Stark decelerator and transported without deceleration over a distance of 100 mm to a second detection region in the apparatus. There, upon switching off the guiding fields, the molecules were detected by PFI at a time $t = 132\ \mu\text{s}$ after photoexcitation. The resulting spectrum is very different to that in Fig. 2(c). It is dominated by the features in the wavenumber range between $30\,400$ and $30\,460\text{ cm}^{-1}$ that are also present in panel (c). However, the spectral intensity distribution is different. The stronger features in the delayed PFI spectrum correspond to excitation on $nf(2)$ resonances, while the transitions to states with $N^+ = 4$ are weaker. Transitions to Rydberg states with $N^+ = 6$ are almost completely absent from this spectrum. They can however be identified in the wavenumber range between $30\,460$ and $30\,510\text{ cm}^{-1}$ if the signal amplitude is scaled by a factor of 15 [orange spectrum inset and vertically offset in panel (b)]. The relative intensities of the observed features arise from a combination of (i) the efficiency with which long-lived Rydberg states were populated, (ii) the efficiency with which the molecules were loaded into, and transported in the traveling electric trap of the decelerator, (iii) the detection efficiency, and (iv) the excited-state decay rates. The gradual reduction in spectral intensity for values of n below ~ 40 is a consequence of the excited states not having sufficiently large electric dipole moments – which scale with n^2 – for efficient guiding. The reduction in the spectral intensity at values of $n \gtrsim 44$ is a consequence of losses by electric field ionization during the guiding process. These losses increase with n because of the n^{-4} -dependence of the ionization electric field strength of high Rydberg states. However, across the spectrum in Fig. 2(b) molecules excited to $n(N^+)$ states with the same value of n are expected to be loaded into, guided in and detected in the decelerator with a similar efficiency because these processes are dominated by the characteristics of the Rydberg

electron charge distribution and not strongly affected by the rotational state of the ion core. The differences in spectral intensity of the series with different values of N^+ in Figs. 2(c) and 2(b) therefore suggest that the molecules prepared in more highly excited rotational states, i.e., those with $N^+ = 4$ and 6, decay more rapidly from the traveling electric traps, as they are guided to the position where delayed PFI was performed, than those in the $N^+ = 2$ states.

Further information on the decay dynamics of the excited molecules was obtained by deceleration to rest in the laboratory-fixed frame of reference and electrostatic trapping. For molecules traveling with an initial longitudinal speed of 795 ms^{-1} this deceleration process took $\sim 250\ \mu\text{s}$.¹⁹ A spectrum recorded with detection after a subsequent trapping time of $50\ \mu\text{s}$, and therefore at total time after photoexcitation of $t = 300\ \mu\text{s}$ is displayed in Fig. 2(a). This spectrum contains fewer strong resonances than that in panel (b). The features observed are predominantly those associated with the transitions to Rydberg states in the $N^+ = 2$ series. This further reduction in signal from molecules in the more highly excited rotational states at this later detection time lends additional weight to the suggestion that for a similar range of values of n , the Rydberg states excited in series converging to more highly excited rotational states of the NO^+ ion core decay more rapidly than those associated with lower rotational states.

Quantitative information on the decay rates of the decelerated and electrostatically trapped molecules was obtained by direct measurements of trap loss. These were carried out for molecules excited on $N^+ = 2$ resonances only, using the methods described and characterized in detail in Ref. 20. This involved measurements of trap decay time constants for values of n between 38 and 44 inclusive, over times ranging from 300 to $600\ \mu\text{s}$ after photoexcitation, i.e., for trapping times between 50 and $350\ \mu\text{s}$. The results of these measurements are presented in Fig. 3(a). Each data point in this figure represents the weighted mean of up to 3 separate measurements. The error bars reported represent the uncertainty on the mean. The measured trap decay time constants range from 340 to $275\ \mu\text{s}$ and generally decrease as the value of n increases. These values agree within the experimental uncertainties with those measured upon photoexcitation from the $A^2\Sigma^+(v^+ = 0, N^+ = 0, J^+ = 1/2)$ intermediate state, reported previously.²⁰ The general decrease in the trap decay time constant with n in this set of data is attributed to the increase in the coupling, as the excitation wavenumber is increased, to the short lived, $\sim 1\text{ ps}$, $n = 7$ states with $v^+ = 1$ located close to the $N^+ = 2$ series limit (see Fig. 1).²⁰ The deviations of the trap decay time constants from this general trend, for example at $n = 43$, can be attributed to effects of intramolecular charge-quadrupole interactions that result in the population of pairs of near degenerate Rydberg states in series with values of N^+ that differ by two.²⁰ In the particular case of the $n = 43$ states in the $N^+ = 2$ series, the coupling that occurs is with the longer-lived near degenerate $n = 48$ states in the $N^+ = 0$ series. The decay time constants of molecules excited to states with $N^+ = 4$ and 6 could not be measured by monitoring loss rates from the electrostatic trap because of the insufficient signal strength at later times after photoexcitation.

Although the decay time constants of $n(4)$ and $n(6)$ Rydberg states could not be obtained from trap decay measurements, they could be determined from the changes in the relative spectral intensities of the corresponding resonances in the spectra recorded at

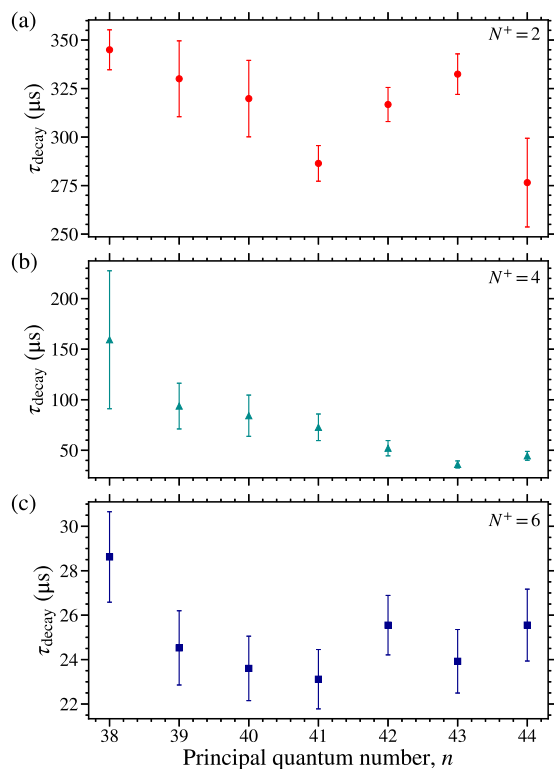


FIG. 3. (a) Measured trap decay time constants, $\tau_{n(2)}$, for NO molecules in long-lived Rydberg states with $N^+ = 2$. Decay time constants determined for molecules in Rydberg-Stark states with (b) $N^+ = 4$, and (c) $N^+ = 6$, from the relative intensities of the corresponding features in spectra recorded upon detection at $t = t_0 = 1 \mu\text{s}$ and $t = t_1 = 132 \mu\text{s}$ after photoexcitation, and calibration using the values of $\tau_{n(2)}$ in panel (a). See text for details.

$t = t_0 = 1 \mu\text{s}$ [Fig. 2(c)] and $t = t_1 = 132 \mu\text{s}$ [Fig. 2(b)] after photoexcitation. To achieve this, the decay rates of the molecules in the $n(2)$ Rydberg states measured after deceleration and electrostatic trapping were used for calibration, and the assumption was made that the decay of the molecules in the time between laser photoexcitation and $t = t_0 = 1 \mu\text{s}$ could be neglected. This is a reasonable assumption in the cases of interest here because this period of time is $<1\%$ of the typical decay time constant of the molecules in these $n(2)$ Rydberg states.

For each value of n , the efficiency with which long-lived Rydberg-Stark states were populated was assumed to be similar for all values of N^+ studied. This assumption is based on the fact that the quantum defects of the optically accessible nf Rydberg states, and hence their proximity to the manifold of long-lived ℓ -mixed Rydberg-Stark states into which population evolves after excitation, are not strongly dependent on the value of N^+ . From this starting point, the differing contributions from the detection and guiding efficiencies in the spectra recorded directly after photoexcitation at $t_0 = 1 \mu\text{s}$, and after confinement and guiding in the traveling trap of the decelerator for $t_1 = 132 \mu\text{s}$, could be accounted for by scaling the data recorded at the later detection time by a factor $C_{\text{scale}}(n, t_1)$, such that the ratio of the resulting, normalized spectral intensity

$C_{\text{scale}}(n, t_1)I_{n(2)}(t_1)$ to $I_{n(2)}(t_0)$ on the $n(2)$ resonances was equal to that expected from an exponentially decaying function with the corresponding decay time constant, $\tau_{n(2)}$, in Fig. 3(a), i.e.,

$$\frac{C_{\text{scale}}(n, t_1)I_{n(2)}(t_1)}{I_{n(2)}(t_0)} = \exp\left[-\frac{t_1 - t_0}{\tau_{n(2)}}\right]. \quad (2)$$

This same scaling factor was used to normalize the signal amplitude associated with the $n(4)$ and $n(6)$ resonances in the same spectrum. The decay rates of these states could then be obtained by determining $\tau_{n(N^+)}$ from

$$\frac{C_{\text{scale}}(n, t_1)I_{n(N^+)}(t_1)}{I_{n(N^+)}(t_0)} = \exp\left[-\frac{t_1 - t_0}{\tau_{n(N^+)}}\right] \quad (3)$$

when $N^+ = 4$ and 6. This procedure was repeated for each individual value of n between 38 and 44 for which the measurements were made, with the results presented in Figs. 3(b) and 3(c).

The data in Figs. 3(b) and 3(c) show that the decay time constants of the $N^+ = 4$ and 6 Rydberg-Stark states populated in the experiments range from 50 to 150 μs , and from 23 to 29 μs , respectively. These are significantly shorter than the values of $\tau_{n(2)}$ in Fig. 3(a). The general trend observed is therefore that the decay time constants for a given value of n reduce as the value of N^+ is increased, i.e., the Rydberg state decay rates increase with increasing N^+ . However, the general trend within each individual N^+ Rydberg series – that the decay time constants decrease as the value of n increases because of interactions of the Rydberg electron with the NO^+ ion core²⁰ – persists for each value of N^+ although it is less apparent for the shorter-lived states with $N^+ = 6$.

The principal new observation reported here is that the decay time constants for Rydberg states excited with the same values of n in NO decrease with rotational excitation of the NO^+ ion core, and in particular that these decay time constants differ by an order of magnitude if N^+ is increased from 2 to 6. The spontaneous emission rates of the Rydberg states studied are not expected to exhibit a strong dependence on N^+ . Therefore the observations point to an increase in the rates of non-radiative decay processes, i.e., rotational autoionization or predissociation, as the value of N^+ increases. Since the $N^+ = 2$ and 4 states studied lie below all lower- N^+ Rydberg series limits (see grey rectangles in Fig. 1), these states cannot decay by rotational autoionization. The change, by a factor of $\sim 1/3$, in the lifetimes of the Rydberg states with $N^+ = 4$ compared to those with $N^+ = 2$ in Figs. 3(a) and 3(b) therefore cannot be attributed to rotational autoionization. As can be seen in Fig. 1, the $N^+ = 6$ Rydberg states studied do lie above the ionization limits of all series with $N^+ \leq 3$. However, the strongest rotational channel interactions that could give rise to rotational autoionization are the charge-dipole interaction between the Rydberg electron and the static electric dipole moment of the NO^+ ion core, and the charge-quadrupole interaction. The charge-dipole interaction couples states for which $\Delta N^+ = 1$, while the charge-quadrupole interaction couples states for which $\Delta N^+ = 0$ or 2. Since couplings between the bound Rydberg states in the $N^+ = 6$ series and the ionization continuum with $N^+ \leq 3$ necessitate an interaction for which $\Delta N^+ \geq 3$ this can only occur through higher-order processes which are not expected to have a high propensity. For the particular states studied here we therefore conclude that the observed dependence of the Rydberg state

decay rates on the value of N^+ is not dominated by effects of rotational autoionization, and must therefore be caused by changes in the Rydberg-state predissociation rates.

Changes in the rates of predissociation of the Rydberg states with $N^+ = 2, 4,$ and 6 studied can be attributed to differences in the amount of low- ℓ character, i.e., $\ell \lesssim 3$, of the Rydberg-Stark states populated in the excitation process as the value of N^+ increases. From the measured decay time constants of the Rydberg states in the $N^+ = 2$ series in Fig. 3(a), and additional data reported in Refs. 20 and 21, we conclude that the molecules in long-lived Rydberg states that are successfully decelerated and trapped must be in states with azimuthal quantum numbers $|M_N| \gtrsim 4$. For $N^+ = 2$, there exist $2N^+ + 1 = 5$ manifolds of ℓ -mixed Rydberg-Stark states, and when $|M_N| = 4$ the minimal short-lived low- ℓ character in each of these manifolds ranges from 2 to 6. Because of this there are many Rydberg-Stark manifolds that do not possess any low- ℓ , i.e., $\ell \lesssim 3$, character. The molecules in these manifolds are therefore most likely to be decelerated and trapped as they are the longest-lived.

This situation is, however, different for $N^+ = 4$ or 6 . For $N^+ = 4$, the manifolds of Rydberg-Stark states for which $|M_N| = 4$ can contain values of ℓ down to zero. The short-lived $\ell \lesssim 3$ character in these manifolds of Rydberg-Stark states, results in shorter measured decay times for each value of n than observed when $N^+ = 2$. For $N^+ = 6$, this situation is even further exaggerated with many more manifolds of $|M_N| = 4$ Rydberg-Stark states possessing low ℓ character, and the decay times of the states populated in the excitation process further reduce. Although the distribution of values of $|M_N|$ of the excited molecules is expected to be similar for each value of N^+ , contributions from states with short-lived low- ℓ character differ significantly as the value of N^+ is increased. The observed reduction in the decay time constants of the molecules for each particular value of n with increasing N^+ is therefore attributed to changes in the underlying low- ℓ character of the states that are populated. This interpretation of the experimental data is consistent with the behavior of the trap decay time constants for a more limited number of Rydberg states with $N^+ = 0, 1,$ and 2 reported in Ref. 20.

IV. CONCLUSIONS

Using a combination of the methods of Rydberg-Stark deceleration and delayed pulsed electric field ionization, effects of rotational excitation of the NO^+ ion core on the decay of long-lived Rydberg states in NO have been studied with unprecedented precision. For a laser photoexcitation scheme that resulted to the population of ℓ -mixed Rydberg-Stark states with similar values of $|M_N|$ for each value of n and N^+ , it was found that in general the decay time constants of the excited states decreased when the NO^+ ion core was more highly rotationally excited. This observation is attributed to an increase in the rates of predissociation of the Rydberg states populated in the experiments as the value of N^+ was increased. This is a consequence of an increase, with the value of N^+ , in the short-lived, predissociative low- ℓ character of the ℓ -mixed Rydberg-Stark states with similar values of $|M_N|$. In the experiments reported, individual Rydberg-Stark states were not resolved spectroscopically or selectively prepared at laser photoexcitation. In future it will be of interest to extend the experiments to achieve full quantum-state resolution, and carry out similar measurements for homonuclear diatomic molecules, e.g., N_2 , in which the absence of an electric dipole

moment of the ion core modifies the strength the charge-multipole interactions that contribute to the observed decay dynamics.

ACKNOWLEDGMENTS

This work was supported by the European Research Council (ERC) under the European Union's Horizon 2020 research and innovation program (Grant No. 683341). M.H.R. is grateful to the Engineering and Physical Sciences Research Council (EPSRC) for support through their Doctoral Training Partnership (Grant No. EP/R513143/1).

AUTHOR DECLARATIONS

Conflict of Interest

The authors have no conflicts to disclose.

Author Contributions

M. H. Rayment: Conceptualization (equal); Formal analysis (equal); Investigation (equal); Methodology (equal); Software (equal); Validation (equal); Visualization (equal); Writing – original draft (equal); Writing – review & editing (equal). **S. D. Hogan:** Conceptualization (equal); Data curation (equal); Funding acquisition (equal); Investigation (equal); Methodology (equal); Project administration (equal); Resources (equal); Supervision (equal); Validation (equal); Visualization (equal); Writing – original draft (equal); Writing – review & editing (equal).

DATA AVAILABILITY

The data that support the findings of this study are available within the article.

REFERENCES

- J. Liu, E. J. Salumbides, U. Hollenstein, J. C. Koelemeij, K. S. Eikema, W. Ubachs, and F. Merkt, "Determination of the ionization and dissociation energies of the hydrogen molecule," *J. Chem. Phys.* **130**, 174306 (2009).
- N. Hölsch, M. Beyer, E. J. Salumbides, K. S. Eikema, W. Ubachs, C. Jungen, and F. Merkt, "Benchmarking theory with an improved measurement of the ionization and dissociation energies of H_2 ," *Phys. Rev. Lett.* **122**, 103002 (2019).
- L. Semeria, P. Jansen, G.-M. Camenisch, F. Mellini, H. Schmutz, and F. Merkt, "Precision measurements in few-electron molecules: The ionization energy of metastable $^4\text{He}_2$ and the first rotational interval of $^4\text{He}_2^+$," *Phys. Rev. Lett.* **124**, 213001 (2020).
- J. Hussels, N. Hölsch, C. F. Cheng, E. J. Salumbides, H. L. Bethlem, K. S. Eikema, C. Jungen, M. Beyer, F. Merkt, and W. Ubachs, "Improved ionization and dissociation energies of the deuterium molecule," *Phys. Rev. A* **105**, 022820 (2022).
- N. Hölsch, I. Doran, M. Beyer, and F. Merkt, "Precision millimetre-wave spectroscopy and calculation of the Stark manifolds in high Rydberg states of para- H_2 ," *J. Mol. Spectrosc.* **387**, 111648 (2022).
- A. Giusti, "A multichannel quantum defect approach to dissociative recombination," *J. Phys. B: At. Mol. Phys.* **13**, 3867 (1980).
- R. Peverall, S. Rosén, J. R. Peterson, M. Larsson, A. Al-Khalili, L. Viktor, J. Semaniak, R. Bobbenkamp, A. Le Padellec, A. N. Maurellis, and W. J. van der Zande, "Dissociative recombination and excitation of O_2^+ : Cross sections, product yields

- and implications for studies of ionospheric airglows," *J. Chem. Phys.* **114**, 6679 (2001).
- ⁸T. P. Softley, "Applications of molecular Rydberg states in chemical dynamics and spectroscopy," *Int. Rev. Phys. Chem.* **23**, 1 (2004).
- ⁹S. L. Guberman, "Role of excited core Rydberg states in dissociative recombination," *J. Phys. Chem. A* **111**, 11254 (2007).
- ¹⁰J. P. Morrison, C. J. Rennick, J. S. Keller, and E. R. Grant, "Evolution from a molecular Rydberg gas to an ultracold plasma in a seeded supersonic expansion of NO," *Phys. Rev. Lett.* **101**, 205005 (2008).
- ¹¹R. Wang, M. Aghigh, K. L. Marroquín, K. M. Grant, J. Sous, F. B. V. Martins, J. S. Keller, and E. R. Grant, "Radio frequency field-induced electron mobility in an ultracold plasma state of arrested relaxation," *Phys. Rev. A* **102**, 063122 (2020).
- ¹²C. H. Greene, A. S. Dickinson, and H. R. Sadeghpour, "Creation of polar and nonpolar ultra-long-range Rydberg molecules," *Phys. Rev. Lett.* **85**, 2458 (2000).
- ¹³V. Bendkowsky, B. Butscher, J. Nipper, J. P. Shaffer, R. Löw, and T. Pfau, "Observation of ultralong-range Rydberg molecules," *Nature* **458**, 1005 (2009).
- ¹⁴R. González-Férez, J. Shertzer, and H. R. Sadeghpour, "Ultralong-range Rydberg bimolecules," *Phys. Rev. Lett.* **126**, 043401 (2021).
- ¹⁵P. Allmendinger, J. Deiglmayr, O. Schullian, K. Höveler, J. A. Agner, H. Schmutz, and F. Merkt, "New method to study ion-molecule reactions at low temperatures and application to the $H_2^+ + H_2 \rightarrow H_3^+ + H$ reaction," *ChemPhysChem* **17**, 3596 (2016).
- ¹⁶P. Allmendinger, J. Deiglmayr, K. Höveler, O. Schullian, and F. Merkt, "Observation of enhanced rate coefficients in the $H_2^+ + H_2 \rightarrow H_3^+ + H$ reaction at low collision energies," *J. Chem. Phys.* **145**, 244316 (2016).
- ¹⁷V. Zhelyazkova, F. B. Martins, J. A. Agner, H. Schmutz, and F. Merkt, "Ion-molecule reactions below 1 K: Strong enhancement of the reaction rate of the ion-dipole reaction $He^+ + CH_3F$," *Phys. Rev. Lett.* **125**, 263401 (2020).
- ¹⁸K. Höveler, J. Deiglmayr, J. A. Agner, H. Schmutz, and F. Merkt, "The $H_2^+ + HD$ reaction at low collision energies: H_3^+/H_2D^+ branching ratio and product-kinetic-energy distributions," *Phys. Chem. Chem. Phys.* **23**, 2676 (2021).
- ¹⁹A. Deller, M. H. Rayment, and S. D. Hogan, "Slow decay processes of electrostatically trapped Rydberg NO molecules," *Phys. Rev. Lett.* **125**, 073201 (2020).
- ²⁰M. H. Rayment and S. D. Hogan, "Quantum-state-dependent decay rates of electrostatically trapped Rydberg NO molecules," *Phys. Chem. Chem. Phys.* **23**, 18806 (2021).
- ²¹M. H. Rayment and S. D. Hogan, "Electrostatic trapping vibrationally excited Rydberg NO molecules," *Mol. Phys.* **121**, e2160846 (2023).
- ²²J. Schmidt, M. Fiedler, R. Albrecht, D. Djekic, P. Schalberger, H. Baur, R. Löw, N. Fruehauf, T. Pfau, J. Anders, E. R. Grant, and H. Kübler, "Proof of concept for an optogalvanic gas sensor for NO based on Rydberg excitations," *Appl. Phys. Lett.* **113**, 011113 (2018).
- ²³J. Schmidt, Y. Münzenmaier, P. Kaspar, P. Schalberger, H. Baur, R. Löw, N. Fruehauf, T. Pfau, and H. Kübler, "An optogalvanic gas sensor based on Rydberg excitations," *J. Phys. B: At., Mol. Opt. Phys.* **53**, 094001 (2020).
- ²⁴M. Seaver, W. A. Chupka, S. D. Colson, and D. Gauyacq, "Double resonance multiphoton ionization studies of high Rydberg states in nitric oxide (NO)," *J. Phys. Chem.* **87**, 2226 (1983).
- ²⁵T. Ebata, Y. Anezaki, M. Fujii, N. Mikami, and M. Ito, "High Rydberg states of nitric oxide studied by two-color multiphoton spectroscopy," *J. Phys. Chem.* **87**, 4773 (1983).
- ²⁶A. Deller and S. D. Hogan, "Excitation and characterization of long-lived hydrogenic Rydberg states of nitric oxide," *J. Chem. Phys.* **152**, 144305 (2020).
- ²⁷P. Lancuba and S. D. Hogan, "Transmission-line decelerators for atoms in high Rydberg states," *Phys. Rev. A* **90**, 053420 (2014).
- ²⁸P. Lancuba and S. D. Hogan, "Electrostatic trapping and *in situ* detection of Rydberg atoms above chip-based transmission lines," *J. Phys. B: At., Mol. Opt. Phys.* **49**, 074006 (2016).
- ²⁹S. N. Dixit, D. L. Lynch, V. McKoy, and W. M. Huo, "Rotational branching ratios in (1+1) resonant-enhanced multiphoton ionization of NO via the $A^2\Sigma^+$ state," *Phys. Rev. A* **32**, 1267 (1985).
- ³⁰H. Rudolph, S. N. Dixit, V. McKoy, and W. M. Huo, "(1+1) resonant enhanced multiphoton ionization via the $A^2\Sigma^+$ state of NO: Ionic rotational branching ratios and their intensity dependence," *J. Chem. Phys.* **88**, 1516 (1988).
- ³¹A. L. Goodgame, H. Dickinson, S. R. Mackenzie, and T. P. Softley, "The Stark effect in the $v^+ = 1$ autoionizing Rydberg states of NO," *J. Chem. Phys.* **116**, 4922 (2002).
- ³²W. A. Chupka, "Factors affecting lifetimes and resolution of Rydberg states observed in zero-electron-kinetic-energy spectroscopy," *J. Chem. Phys.* **98**, 4520 (1993).
- ³³F. Merkt and R. N. Zare, "On the lifetimes of Rydberg states probed by delayed pulsed field ionization," *J. Chem. Phys.* **101**, 3495 (1994).
- ³⁴M. J. J. Vrakking and Y. T. Lee, "Lifetimes of Rydberg states in zero-electron-kinetic-energy experiments. I. Electric field induced and collisional enhancement of NO predissociation lifetimes," *J. Chem. Phys.* **102**, 8818 (1995).
- ³⁵M. Bixon and J. Jortner, "The dynamics of predissociating high Rydberg states of NO," *J. Chem. Phys.* **105**, 1363 (1996).
- ³⁶M. J. Vrakking and Y. T. Lee, "Enhancements in the lifetimes of NO Rydberg states in dc electric fields: Implications for zero-electron-kinetic-energy photoelectron spectroscopy experiments," *Phys. Rev. A* **51**, R894 (1995).
- ³⁷S. D. Hogan, "Rydberg-Stark deceleration of atoms and molecules," *EPJ Tech. Instrum.* **3**, 2 (2016).
- ³⁸R. Patel, N. J. Jones, and H. H. Fielding, "Observation of the Stark effect in $v^+ = 0$ Rydberg states of NO with a matrix-diagonalization analysis," *J. Phys. B: At., Mol. Opt. Phys.* **40**, 1369 (2007).
- ³⁹M. Bixon and J. Jortner, "Intramolecular coupling between non-penetrating high molecular Rydberg states," *Mol. Phys.* **89**, 373 (1996).